12-1-2000

Surface segregation and restructuring of colossal-magnetoresistant manganese perovskites $La_{0.65}Sr_{0.35}MnO_3$

Hani Dulli
University of Tennessee, Knoxville, hani.dulli@uconn.edu

Peter A. Dowben
University of Nebraska-Lincoln, pdowben@unl.edu

Sy-Hwang Liou
University of Nebraska-Lincoln, sliou@unl.edu

E. Ward Plummer
University of Tennessee, Knoxville, wplummer@phys.lsu.edu

PHYSICAL REVIEW B VOLUME 62, NUMBER 22 1 DECEMBER 2000-II

Surface segregation and restructuring of colossal-magnetoresistant manganese perovskites $La_{0.65}Sr_{0.35}MnO_3$

Hani Dulli,[1] P. A. Dowben,[2] S.-H. Liou,[2] and E. W. Plummer[1]
[1]*Department of Physics and Astronomy, University of Tennessee, Knoxville, Tennessee 37996 and Solid State Division, Oak Ridge National Laboratory, Oak Ridge, Tennessee 37831*
[2]*Department of Physics and Astronomy and the Center for Materials Research and Analysis, Behlen Laboratory of Physics, University of Nebraska–Lincoln, Lincoln, Nebraska 68588*
(Received 23 May 2000)

We have investigated the surface chemical composition of crystalline films of $La_{0.65}Sr_{0.35}MnO_3$ by angle-resolved x-ray photoelectron spectroscopy. The surface composition was found to be significantly different from that of the bulk because of an appreciable Sr segregation. Furthermore, our study suggests that this Sr segregation has caused a major restructuring of the surface region characterized by the formation of a Ruddlesden-Popper phase $(La,Sr)_{n+1}Mn_nO_{3n+1}$ with $n=1$. Segregation and restructuring in the surface region should be common in these doped perovskites and will have a profound impact on the electronic and magnetic properties of ultrathin films and magnetic tunneling junctions made of these materials.

Transition metal oxides (TMO's) of perovskite structure show a rich variety of properties originating from the mutual coupling between spin, charge, and lattice degrees of freedom. These properties include, for instance, colossal magnetoresistance (CMR), metal-insulator transition, and charge and spin ordering.[1] Due to their chemical stability as well as the almost common lattice spacing, these materials are quite suitable for the fabrication of heterostructures and superlattices aimed at developing a new generation of materials with tailored magnetoelectronic properties.[2] Such interest in artificially layered structures is inevitably drawing more attention to the properties of the surface and interface regions.

The creation of a surface breaks the symmetry of a crystal inducing various electronic, magnetic, and geometrical changes. As a result of these changes the surface free energy will be different from that of the bulk, driving surface segregation and therefore changing the chemical composition of the surface region. Since the phase diagram of most TMO's is critically dependent upon the doping concentration, the surface could be a ''different material.'' Thus a thorough knowledge of the surface composition and structure is of primary importance for understanding the electronic and magnetic properties of TMO's surfaces and interfaces.

Surface segregation phenomena are more the rule than the exception, as witnessed in many systems by studies of binary alloys.[3] Similar phenomena are present in oxides, but only a few experimental and theoretical studies have addressed the issue.[4] The different surface free energies (surface bond breaking) of the elements and the different atomic sizes (lattice strain) makes it possible to reduce the free energy of the system by having one or the other of the elements segregate. Furthermore, surface segregation should be expected in metal oxides of ionic nature because of the existence of a space-charge layer in the near surface region, providing a strong chemical potential to drive segregation.[5] Surface segregation studies have proven to be important for studies of catalysis, corrosion, joining, etc. Since the physical properties of the TMO's are so sensitive to the structure and dopant concentration, segregation studies in this class of materials are essential.

We have studied the surface chemical composition of crystalline films of $La_{0.65}Sr_{0.35}MnO_3$ by angle-resolved x-ray photoelectron spectroscopy (ARXPS). The surface composition was found to be quite different from that of the bulk with clear evidence of Sr surface segregation. Furthermore, our data is only explainable if a major restructuring of the surface region characterized by the formation of a Ruddlesden-Popper phase $(La,Sr)_{n+1}Mn_nO_{3n+1}$ with $n=1$ occurs.

$La_{1-x}Sr_xMnO_3$ ($x=0.35$) thin films (nominal thickness of 1000 Å) were grown on (100) $LaAlO_3$ substrates by rf sputtering in a 2:1 argon/oxygen atmosphere maintained at 20 mTorr. The substrate was maintained at a temperature of 700 °C throughout the growth process. The films were subsequently annealed at 900 °C in an oxygen atmosphere of 2 atm for 10 h. The bulk chemical composition of the films was determined from energy dispersive analysis of x-ray emission spectroscopy (XES or EDAX) and found to be similar to the targets with the final compositions $La_{0.65}Sr_{0.35}MnO_3$. The crystallinity and orientation were established by x-ray diffraction which indicates that the surface normal is aligned with the *c* axis. The electronic and magnetic properties were determined with temperature dependent resistivity and magnetization measurements which show a Curie temperature of 370 K consistent with measurement of bulk samples.[1] Samples were cleaned *in situ* by repeated annealing and exposure to low-energy electrons to stimulate the desorption of contaminants. Appropriate surface preparation was established by x-ray photoelectron spectroscopy (XPS), ultraviolet photoemission, and inverse photoemission. Prior to each experiment, samples were again cleaned by annealing at 500 °C for 2 h. Although no low-energy electron diffraction (LEED) pattern could be obtained from the film's surface, a highly dispersive band with apparent periodic dispersion was observed in the inverse photoemission spectroscopy (IPES) study.[6] The implication is that even though the immediate surface layer is disordered the film's selvage region must be ordered and consequently the band

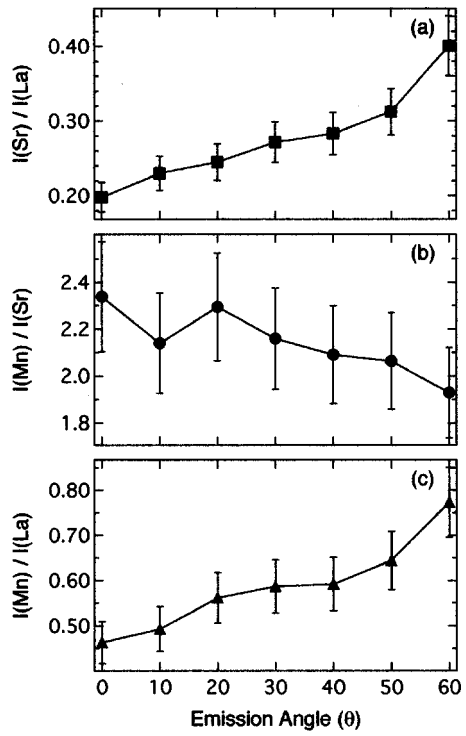

FIG. 1. Relative intensities of (Sr $3d_{5/2}$+Sr $3d_{3/2}$) to La $3d_{5/2}$, Mn $2p_{3/2}$ to (Sr $3d_{5/2}$+Sr $3d_{3/2}$), and Mn $2p_{3/2}$ to La $3d_{5/2}$ all as functions of the emission angle.

seen in the inverse photoemission penetrates deeper into the solid than the LEED beam. XPS measurements were performed with Mg $K\alpha$ (1253.6 eV) radiation from a PHI Model 04-548 Dual Anode x-ray source. Energy distribution curves of the elemental core levels were acquired with a hemispherical electron energy analyzer (PHI Model 10-360 Precision Energy Analyzer) with an acceptance angle of $\pm 7°$. The core level spectra were measured at a pass energy of 23.5 eV. ARXPS has been used for the nondestructive determination of composition depth profiles in the surface region. This technique has been utilized in many studies focused on the investigation of surface segregation in different systems.[7]

Figure 1 shows plots of three relative intensities: (a) (Sr $3d_{5/2}$+Sr $3d_{3/2}$) to La $3d_{5/2}$, (b) Mn $2p_{3/2}$ to (Sr $3d_{5/2}$ +Sr $3d_{3/2}$), and (c) Mn $2p_{3/2}$ to La $3d_{5/2}$ as a function of the emission angle. We will call these three ratios simply Sr/La, Mn/Sr, and Mn/La, respectively. First notice the strong angular dependence of Sr/La ratio. If the relative concentration of Sr with respect to that of La was independent of the depth into the sample the Sr/La ratio would be roughly constant. It is clear from Fig. 1(a) that this ratio is not constant but it is increasing with increasing emission angle. Qualitatively this shows that the surface region is Sr rich, or in other words, Sr has segregated to the surface. Figure 1(b) shows a fairly small decrease in Mn/Sr ratio, which can be also attributed to the increase in surface concentration of Sr. The Mn/La ratio is increasing with the emission angle [Fig. 1(c)] indicating a deficiency of La near the surface and giving further evidence of Sr segregation. The XPS data will be used to quantitatively analyze the surface composition altered by Sr segregation.

The angular dependence of the core levels' intensities can yield quantitative information about the surface composition of solids.[8] The XPS intensity ratio $R_{AB}(\theta)$ of two core level peaks (used to identify two elements of A and B) is defined as

$$R_{AB}(\theta)=\frac{\sigma_A}{\sigma_B}\frac{T_A}{T_B}\frac{\sum_i f_i^A \exp\left(\frac{-id}{\lambda_A\cos(\theta)}\right)}{\sum_j f_j^B \exp\left(\frac{-jd}{\lambda_B\cos(\theta)}\right)}, \tag{1}$$

where σ is the photoionization cross section, T is the transmission coefficient of the analyzer, f_i^A is the atomic fraction of element A at the ith layer, f_j^B is the atomic fraction of element B at the jth layer, d is the interlayer spacing, λ is the inelastic mean free path of the emitted electrons, and θ is the emission angle with respect to the surface normal. The cross sections were taken from Scofield's calculations for an excitation energy of 1253.6 eV (Mg $K\alpha$) (Ref. 9) (5.29 for Sr $3d$, 26.49 for La $3d_{5/2}$, and 8.99 for Mn $2p_{3/2}$). The transmission coefficient of our analyzer varies as the inverse of the kinetic energy of the emitted electrons.[10] The mean free paths of the electrons in the material were calculated according to the scheme of Tanuma *et al.*[11] ($\sim$20 Å for Sr $3d$, $\sim$10 Å for La $3d_{5/2}$, and $\sim$13 Å for Mn $2p_{3/2}$). The Sr atomic fraction f_i^{Sr} has been fitted with an assumed exponential segregation profile:

$$f_i^{\mathrm{Sr}}=b+\delta e^{-id/G}, \tag{2}$$

where b is the bulk fraction of Sr in the material (0.35 in our case), δ and G are two parameters reflecting the extent of segregation and can be determined by finding the best fit to the measured intensity ratio. The other atomic fractions can be simply written in the following way:

$$f_i^{\mathrm{La}}=1-f_i^{\mathrm{Sr}}, \quad f_j^{\mathrm{Mn}}=1. \tag{3}$$

Finally, the values of the summation indices i and j are dictated by the stacking sequence. The fitting procedure was the following: (1) assume a certain stacking sequence, (2) fit the Sr/La experimental ratio by adjusting δ and G, (3) calculate the Mn/Sr and Mn/La ratios given the fit to the Sr/La ratio, and (4) if the calculated ratios of the previous steps do not fit the corresponding experimental ones, then try a new stacking sequence.

The first attempt to fit the data assumes the perovskite structure of the bulk with La/SrO termination because this surface is nonpolar. The blue dashed line in Fig. 2(a) is the best fit of the (Sr/La) data for this termination with δ=0.60 and G=3.5. Using these parameters, we calculate (Mn/Sr) ratio [dashed borderline of the blue hatched region in Fig. 2(b)] and (Mn/La) ratio [dashed borderline of the blue hatched region in Fig. 2(c)]. It is clear that these two calculated ratios do not provide a reasonable fit to the corresponding experimental data. Next, the perovskite structure has been chosen with MnO_2 termination which is polar surface unless the next layer is 100% Sr so that all of the Mn ions are Mn^{4+}. An equally good fit (δ=0.72,G=3.6) has been obtained to the (Sr/La) data [same blue dashed line in Fig. 2(a)]. However, the calculated ratios of (Mn/Sr) and (Mn/La) [solid borderlines of the blue hatched regions in Fig. 2(b) and Fig. 2(c), respectively] are far from being good fits to the

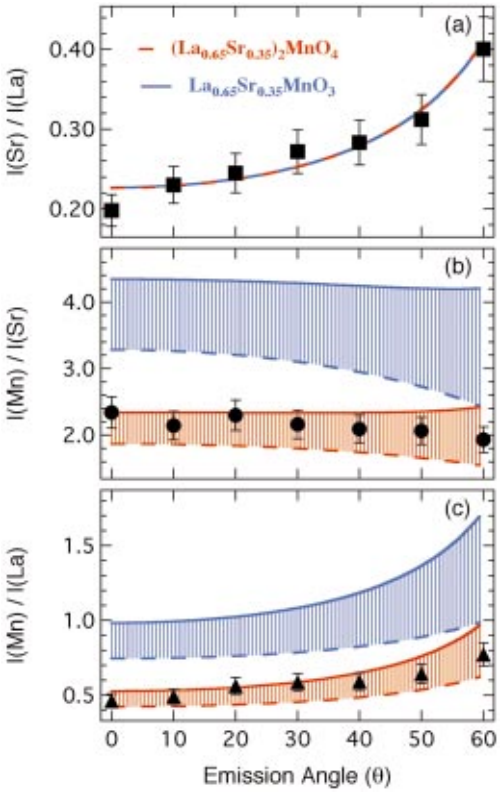

FIG. 2. (Color) Part (a) shows the best fit of (Sr/La) data for the possible stacking sequences of $La_{0.65}Sr_{0.35}MnO_3$ structure (blue dashed line) and that of $(La_{0.65}Sr_{0.35})_2MnO_4$ structure (red dashed line). The corresponding calculated ratios of (Mn/Sr) and (Mn/La) for $La_{0.65}Sr_{0.35}MnO_3$ ($(La_{0.65}Sr_{0.35})_2MnO_4$) structure are shown as blue (red) hatched regions in parts (b) and (c), respectively, where the dashed borderlines correspond to La/SrO termination and the solid borderlines correspond to MnO_2 termination.

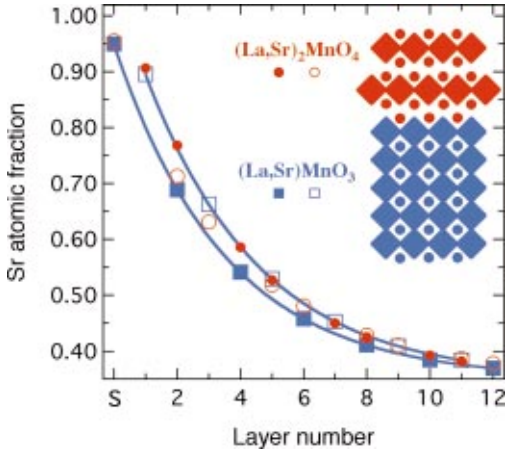

FIG. 3. (Color) The blue solid (open) squares represent the Sr atomic fraction per layer for the perovskite structure of $La_{0.65}Sr_{0.35}MnO_3$ with La/SrO (MnO_2) termination. The red open (solid) circles represent the Sr atomic fraction for the K_2NiF_4 structure of $(La_{0.65}Sr_{0.35})_2MnO_4$ with La/SrO (MnO_2) termination.

experimental data. Even a mixed terminated surface will not provide a basis to fit the (Mn/Sr) and (Mn/La) data as seen from the blue hatched regions in Fig. 2(b) and Fig. 2(c). It is abundantly clear that there is something fundamentally wrong. It looks like there is about $\frac{1}{2}$ of the Mn present in the surface region as expected from the perovskite structure. However, a more realistic picture is that we have a structure in the surface region with twice the number of (La,Sr) atoms compared to what we have in the bulk. Thus the reconciliation of the experimental data with an appropriate stacking sequence is possible by restructuring the surface region such that it becomes $(La_{0.65}Sr_{0.35})_2MnO_4$ (K_2NiF_4 structure) on top of $La_{0.65}Sr_{0.35}MnO_3$ of the bulk (see the inset in Fig. 3). We believe that the desire of this system to segregate Sr to the surface drives the restructuring which will accumulate more Sr in the surface region. Indeed, by considering the structure of $(La_{0.65}Sr_{0.35})_2MnO_4$, the different experimental ratios in Fig. 2 can be fitted as seen from the red dashed line in part (a) and the red hatched regions in parts (b) and (c) of that figure. The dashed borderlines of the red hatched regions in Fig. 2(b) and Fig. 2(c) correspond to La/SrO termination, whereas the solid borderlines correspond to MnO_2 termination. We believe that the surface is composed of terraces with La/SrO but with many steps exposing the MnO_2 layer just beneath it as seen by ARXPS and effectively making the surface look like a mixed terminated one. Among many stacking sequences considered in the calculations, only one other sequence seems to fit the experimental data of Fig. 2, which is that of $(La_{0.65}Sr_{0.35})_3Mn_2O_7$ with La/SrO termination. Therefore, we would not rule out the possibility of having this ($n=2$) Ruddlesden-Popper phase in the surface region.

The Sr atomic fraction can now be plotted as a function of layer number using Eq. (2) as shown in Fig. 3. The blue solid (open) squares represent the Sr atomic fraction per layer for the perovskite structure of $La_{0.65}Sr_{0.35}MnO_3$ with La/SrO (MnO_2) termination. The red open (solid) circles represent the Sr atomic fraction for the K_2NiF_4 structure of $(La_{0.65}Sr_{0.35})_2MnO_4$ with La/SrO (MnO_2) termination. We see that there is a significant surface segregation of Sr to the near surface region. In fact, according to this fitting procedure the first layer that contains Sr, whether it is the topmost layer or the one just beneath it, is almost a full SrO layer. Consequently, the first plane of Mn is almost all of the Mn^{4+} ions. The segregation profile of Fig. 3 was found to be stable over the temperature range 180–300 K.

One of the characteristics of transition metal oxides that is distinctly different from those of metals and semiconductors is the ability to accommodate stoichiometry variations by forming thermodynamically stable structures.[12] Actually, perovskites (ABO_3) differ from many materials by resisting the formation of point defects when they become nonstiochiometric.[13] Instead, they form Ruddlesden-Popper phases of the general formula $A_{n+1}B_nO_{3n+1}$.[14] Strontium titanates ($SrTiO_3$) is known for such behavior as have been indicated by various theoretical[15] and experimental studies.[14] Also, the surface of this perovskite was found drastically altered for both oxidized (800–1000 °C, 200 Torr O_2) and reduced crystals (1000 °C, 10^{-8} Torr O_2) in comparison with the stoichiometric bulk.[16] It was concluded that such changes have to be interpreted in terms of segregation processes and solid-state reactions at elevated temperatures which cause the formation of chemical phases in the surface region.[16]

In conclusion, the surface region of $La_{0.65}Sr_{0.35}MnO_3$ was found to be compositionally and structurally quite different from the bulk. These differences will influence the surface properties of these CMR perovskites leading in particular to distinct surface electronic[6] as well as magnetic properties of this important class of transition metal oxides. The surface segregation of the dopant atoms in these manganese perovskite thin films is not restricted to Sr. Other studies show that this phenomenon exists in $La_{0.65}D_{0.35}MnO_3$ (D=Ca,Sr,Pb);[17,18] however, surface restructuring by the formation of a Ruddlesden-Popper phase is found not viable in the case of Ca doped films.[18]

The primary support for this work came from the Joint Center for Atom Technologies (JRCAT) through the Atomic Technology Partnership. P.A.D.'s effort was also supported by NSF (Grant No. DMR-98-02126) and the Center for Materials Research and Analysis (CMRA) at the University of Nebraska.

[1] M. Imada, A. Fujimori, and Y. Tokura, Rev. Mod. Phys. **70**, 1039 (1998).
[2] M. Izumi, Y. Murakami, Y. Konishi, T. Manako, M. Kawasaki, and Y. Tokura, Phys. Rev. B **60**, 1211 (1999).
[3] P. M. Ossi, Surf. Sci. **201**, L519 (1988); F. F. Abraham and C. R. Brundle, J. Vac. Sci. Technol. **18**, 506 (1981).
[4] V. E. Henrich and P. A. Cox, *The Surface Science of Metal Oxides* (Cambridge University Press, Cambridge, 1994).
[5] K. L. Kliewer and J. S. Koehler, Phys. Rev. **140**, A1226 (1965).
[6] H. Dulli, P. A. Dowben, J. Choi, S.-H. Liou, and E. W. Plummer, Appl. Phys. Lett. **77**, 570 (2000).
[7] P. R. Webber, C. E. Rojas, P. J. Dobson, and D. Chadwick, Surf. Sci. **105**, 20 (1981); J. M. Grimal and P. Marcus, *ibid*. **249**, 171 (1991).
[8] V. I. Nefedov and O. A. Baschenko, J. Electron Spectrosc. Relat. Phenom. **47**, 1 (1988).
[9] J. H. Scofield, J. Electron Spectrosc. Relat. Phenom. **8**, 129 (1976).
[10] Technical Manual of PHI Model 10-360 Precision Energy Analyzer.
[11] S. Tanuma, C. J. Powell, and D. R. Penn, Surf. Interface Anal. **21**, 165 (1994).
[12] D. A. Bonnell, Prog. Surf. Sci. **57**, 187 (1998); J. Am. Ceram. Soc. **81**, 3049 (1998).
[13] R. J. D. Tilley, J. Solid State Chem. **21**, 293 (1977).
[14] N. J. Cockroft, S. H. Lee, and J. C. Wright, Phys. Rev. B **44**, 4117 (1991).
[15] K. R. Udayakumar and A. N. Cormack, J. Phys. Chem. Solids **50**, 55 (1989); J. Am. Ceram. Soc. **71**, C-469 (1988).
[16] K. Szot and W. Speier, Phys. Rev. B **60**, 5909 (1999).
[17] J. Choi, J. Zhang, S.-H. Liou, P. A. Dowben, and E. W. Plummer, Phys. Rev. B **59**, 13 453 (1999).
[18] H. Dulli, J. Choi, C. Borca, S.-H. Liou, P. A. Dowben, and E. W. Plummer (unpublished).